

A microRNA Expression-based Model Indicates Event Free Survival In Pediatric Acute Myeloid Leukemia

Lim, et al

Supplementary Information

Table of Contents

Supplementary Experimental Procedures	4
Patient Samples	4
Cytogenetic Risk Assessments	4
Library construction and sequencing of miRNA-seq Illumina libraries	4
Library construction and sequencing of mRNA-seq Illumina libraries	4
Novel miRNA Discovery	5
mRNA isoform-specific expression profiling of mRNA-seq	6
NMF clustering of miRNA expression	6
Differential expression analysis	6
Integrative miRNA:mRNA expression analysis	6
Survival analysis	7
Development of the miRNA-based EFS predictive model	8
Cell line	9
Plasmid constructs and miRNA mimics	9
Dual-Luciferase reporter assays	10
Supplementary Figures	11
Supplementary Figure S1 – miRNA k2-15 NMF metrics	11
Supplementary Figure S2 – miR-106a expression in the Discovery Cohort	13
Supplementary Figure S3 – miRNA with linear associations with patient overall survival (OS) and event free survival (EFS) in both the Discovery Cohort and AAML1031 Validation Cohort	14
Supplementary Figure S4 – Identifying miRNA:mRNA expression correlations	16
Supplementary Figure S5 – AAML0531 Patient EFS (Grouped By Consolidation Therapy)	18
Supplementary Figure S6 – Cytogenetic/molecular Standard Risk cases are further classified by AMLmiR36	19
Supplementary Figure S7 – Median miRNA Expression	21
References For Supplementary Information	22

Supplementary Experimental Procedures

Patient Samples

Karyotyping was centrally reviewed by each study group. Consent was obtained from all study participants in accordance with the Declaration of Helsinki. Institutional review board approval was obtained by the Fred Hutchinson Cancer Research Centre and the COG Myeloid Disease Biology Committee before analysis.

Cytogenetic Risk Assessments

Cytogenetic and molecular abnormalities were used to stratify patients into risk groups^{1,2}. The low risk group included patients with core-binding factor AML [t(8;21) or inv(16)/t(16;16)] and/or *NPM1* or *CEBPA* mutations without *FLT3*-ITD mutations. The high risk group included patients with high allelic ratio (0.4), *FLT3*-ITD+ and/or monosomy 5, del(5q), or monosomy 7. The remaining patients with known cytogenetics were designated as intermediate risk.

Library construction and sequencing of miRNA-seq Illumina libraries

RNA extraction, miRNA-seq library construction, sequencing, read alignment and miRNA expression profiling was performed as previously reported^{3,4}. miRNA-seq reads were aligned to hg19 and mirBase v21, and miRNA 3p/5p strands that were expressed at a level of at least 10 reads per million mapped reads (RPM) in at least 10 libraries were retained for analysis.

Library construction and sequencing of mRNA-seq Illumina libraries

PolyA+ RNA was purified using the 96-well MultiMACS mRNA isolation kit on the MultiMACS 96 separator (Miltenyi Biotec, Germany) from 2µg total RNA with on-column DNaseI-treatment as per the manufacturer's instructions. The eluted PolyA+ RNA was ethanol precipitated and resuspended in 10µL of DEPC treated water with 1:20 SuperaseIN (Life Technologies, USA).

First-strand cDNA for mRNA-seq was synthesized from the purified polyadenylated messenger RNA using Superscript II Reverse Transcriptase (Thermo-Fisher, USA). Second strand cDNA was synthesized following the Superscript cDNA

Synthesis protocol by replacing the dTTP with dUTP in dNTP mix, allowing the second strand to be digested using UNG (Uracil-N-Glycosylase, Life Technologies, USA) in the post-adaptor ligation reaction and thus achieving strand specificity.

cDNAs were fragmented using Covaris E210 sonication for 55 seconds at a “Duty cycle” of 20% and “Intensity” of 5. Paired-end sequencing libraries were prepared following the BC Cancer Agency Genome Sciences Centre strand-specific, plate-based and paired-end (PE) library construction protocols on a Biomek FX robot (Beckman-Coulter, USA). Briefly, cDNA was purified in 96-well format using Ampure XP SPRI beads, and was subject to end-repair and phosphorylation using T4 DNA polymerase, Klenow DNA Polymerase, and T4 polynucleotide kinase respectively in a single reaction, followed by SPRI bead cleanup and 3' A-tailing using Klenow fragment (3' to 5' exo minus). Illumina PE adapters were ligated and the adapter-ligated products were purified using Ampure XP SPRI beads, and digested with UNG (1U/ μ L) at 37°C for 30 min followed by deactivation at 95°C for 15 min. The digested cDNAs were purified using Ampure XP SPRI beads, and then PCR-amplified with Phusion DNA Polymerase (Thermo Fisher Scientific, USA) using Illumina’s PE primer set, with cycle conditions 98°C for 30 sec followed by 10-13 cycles of 98°C for 10 sec, 65°C for 30 sec and 72°C for 30 sec, and finally 72°C for 5 min. The PCR products were purified using Ampure XP SPRI beads, and checked with Caliper LabChip GX for DNA samples using the High Sensitivity Assay (PerkinElmer, USA). PCR products of the desired size range were purified using SPRI beads, and the DNA quality was assessed and quantified using an Agilent DNA 1000 series II assay and Quant-iT dsDNA HS Assay Kit using a Qubit fluorometer (Invitrogen), then diluted to 8nM in preparation for Illumina HiSeq2500 paired-end 75 base sequencing.

Novel miRNA Discovery

In order to identify miRNAs that were not previously reported in mirBase (version 21), we performed novel miRNA discovery using mirDeep2. Shortlisted putative novel miRNA species were those that: 1) had mirDeep2 scores of ≥ 10 in ≥ 10 miRNA-seq libraries, 2) were not predicted by mirDeep2 to be other types of RNA (eg. rRNA, tRNA, snoRNA, etc.), 3) did not have genomic coordinates that intersected with UCSC genome browser annotation tracks using bedtools.

mRNA isoform-specific expression profiling of mRNA-seq

The mRNA-seq paired-end reads were aligned to the RefSeq hg19 reference genome using TopHat v1.4.1^{1,5}. Alignments were then interrogated for isoform-specific expression profiles using Cufflinks v1.3.0^{1,2,5}. mRNA transcripts with at least 1 fragment per kilobase of transcript per million mapped reads (FPKM) in 1 mRNA-seq library were considered expressed and were retained for analysis.

NMF clustering of miRNA expression

Only primary samples were included in the NMF clustering analysis. We generated unsupervised consensus clustering results as previously described^{3,4}. We used the default Brunet algorithm and 100 iterations for the clustering runs. A preferred cluster result was selected by considering the profiles of the cophenetic scores of the consensus membership matrix for clustering solutions having between 2 and 15 clusters.

We chose the 4-group (k=4) solution as it had the second highest cophenetic score and produced a visually clean consensus matrix when compared with the other solutions (Supplementary Figure S1). We chose the 4-group solution over the 2-group solution, which had the higher cophenetic score, reasoning that the 4-group solution would uncover more insight into the heterogeneity miRNA expression in pediatric AML. This proved to be true as we observed significant enrichment of clinical characteristics in all 4 subgroups (Figure 2C). Enrichment of particular clinical characteristics in each subgroup was determined using Fisher's exact tests, where significant enrichment was reported if p-value <0.05.

Differential expression analysis

Evaluation of the differential expression of miRNA was performed using the Wilcoxon ranked-sum test for each miRNA. We considered significantly differentially expressed miRNAs to be those with Benjamini-Hochberg (BH) multiple test corrected p-values (q-values)<0.05.

Integrative miRNA:mRNA expression analysis

Integrative miRNA:mRNA analysis was performed as previously described^{1,2,5}. We considered samples for which we had both miRNA-seq and mRNA-seq data

(n=164). Briefly, a Spearman correlation coefficient (ρ) score and a p-value were generated for comparisons of expression profiles between all possible miRNA and mRNA pairs. Then, miRNA:mRNA pairs were shortlisted based on the presence of target site predictions (from both TargetScan and miRanda algorithms) and significant anti-correlation between miRNA and gene expression, with statistical significance determined from comparing against bootstrapping-based null distributions (Supplementary Figure S4).

KEGG pathway enrichment of target genes of miRNAs was performed using the Fisher's exact test. The groups of miRNAs we considered were: (1) miRNAs that were abundantly expressed in refractory samples vs primary samples; (2) miRNAs that were poorly expressed in refractory samples vs primary samples; (3) miRNAs that were abundantly expressed in relapse samples vs primary samples, and (4) miRNAs that were poorly expressed in relapse samples vs primary samples. Significantly enriched pathways were those with BH multiple test corrected p-values (q-values) < 0.05 .

Survival analysis

Overall survival (OS) was measured from the date of registration to the date of death due to any cause, with patients last known to be alive censored at the date of last contact. Event free survival (EFS) was measured from the date of registration to the date of the first of the following events: removal from protocol therapy without achieving CR, progression, or death due to any cause. Patients who were last known to be alive and progression free were censored at the date of last contact.

For each miRNA, we performed Cox proportional hazards (PH) analysis using the Survival R package, where (1) Low/High expression groups or (2) Reads per million mapped reads (RPM) values were used as input. Significant associations with survival were those with Benjamini-Hochberg (BH) multiple test corrected p-values (q-values) <0.05 . We used X-tile cohort separation^{3, 4} to categorize patients into Low/High expression groups based on Event Free Survival (EFS) data. A cut point was then determined by taking a mean of the maximum value in the low group and minimum value in the high group. This method for determining the cut-point was used as it resulted in the Kaplan-Meier separation with the lowest p-value. The p-value displayed on each

Kaplan-Meier plot is a log-rank p-value. This cut-point was determined in the Discovery Cohort and carried over to the analysis of the AAML1031 Validation Cohort.

For multivariate analyses, we performed Cox PH analysis using the following as input: 1) Low/High expression groups, 2) risk group status, 3) white blood cell count status (>100 or <100). miRNAs that were associated with survival independently of Risk Group assignments (Low Risk or High Risk) or white blood cell (WBC) count status were those with multivariate Cox PH p-values <0.05. Only patients with no missing cytogenetic risk group and WBC information were included for multivariate analyses.

Development of the miRNA-based EFS predictive model

The miRNA-based EFS predictive model was derived based on the data from the Discovery (Training) cohort, and then applied to the Discovery (Test) Cohort and AAML1031 Validation Cohort. miRNA expression (\log_2 RPM), WBC cell count status (>100 or <100), and cytogenetic risk group assignments (Low Risk or High Risk) were used as input features. The glmnet (R package) lasso Cox regression algorithm returned a model score for each patient in the training cohort and non-zero regression coefficients for each significant miRNA feature. Glnet returned 36 miRNAs with non-zero coefficients, and these miRNA feature coefficients were retained in our model.

Model scores for each patient are calculated by multiplying each of the 36 miRNA feature coefficients by its corresponding \log_2 RPM expression value, and then taking the sum of each of these products:

$$\begin{aligned} \text{Patient Model Score} = & -0.071435852 * [\text{hsa-miR-409-5p } \log_2 \text{RPM}] + \\ & -0.063621683 * [\text{hsa-miR-139-5p } \log_2 \text{RPM}] + \\ & -0.062530666 * [\text{hsa-let-7g-5p } \log_2 \text{RPM}] + \\ & -0.062192126 * [\text{hsa-miR-375 } \log_2 \text{RPM}] + \\ & -0.059026016 * [\text{hsa-miR-2110 } \log_2 \text{RPM}] + \\ & -0.050372946 * [\text{hsa-miR-146a-5p } \log_2 \text{RPM}] + \\ & -0.048514515 * [\text{hsa-miR-202-5p } \log_2 \text{RPM}] + \\ & -0.047275703 * [\text{hsa-miR-1180-3p } \log_2 \text{RPM}] + \\ & -0.04528897 * [\text{hsa-miR-335-3p } \log_2 \text{RPM}] + \\ & -0.040989372 * [\text{hsa-miR-181c-3p } \log_2 \text{RPM}] + \\ & -0.040306357 * [\text{hsa-miR-217 } \log_2 \text{RPM}] + \\ & -0.037325674 * [\text{hsa-miR-539-5p } \log_2 \text{RPM}] + \\ & -0.032959784 * [\text{hsa-miR-664b-5p } \log_2 \text{RPM}] + \\ & -0.02419678 * [\text{hsa-miR-1287-3p } \log_2 \text{RPM}] + \\ & -0.019307849 * [\text{hsa-miR-4662a-5p } \log_2 \text{RPM}] + \\ & -0.018062943 * [\text{hsa-miR-148b-3p } \log_2 \text{RPM}] + \end{aligned}$$

-0.011324553*[hsa-miR-181c-5p log₂RPM] +
-0.003799344*[hsa-miR-340-3p log₂RPM] +
-0.002882947*[hsa-miR-132-3p log₂RPM] +
-0.001863252*[hsa-miR-100-5p log₂RPM] +
0.005215312*[hsa-miR-362-3p log₂RPM] +
0.006792342*[hsa-miR-363-3p log₂RPM] +
0.010667128*[hsa-miR-181b-3p log₂RPM] +
0.013641305*[hsa-miR-502-3p log₂RPM] +
0.013849354*[hsa-miR-935 log₂RPM] +
0.015230088*[hsa-miR-296-5p log₂ RPM] +
0.015253859*[hsa-miR-450a-5p log₂RPM] +
0.017215965*[hsa-miR-30e-3p log₂RPM] +
0.018074572*[hsa-miR-30c-2-3p log₂RPM] +
0.027657901*[hsa-miR-34c-5p log₂RPM] +
0.03910599*[hsa-miR-320a log₂RPM] +
0.042520575*[hsa-miR-130b-3p log₂RPM] +
0.06433791*[hsa-miR-155-5p log₂RPM] +
0.070234817*[hsa-miR-1247-3p log₂RPM] +
0.155286578*[hsa-miR-584-5p log₂RPM] +
0.244530267*[hsa-miR-106a-3p log₂RPM]

Optimal model score cut-points for assigning patients into high, intermediate and low model score groups were determined in the Discovery (Training) Cohort. This was accomplished by identifying the cut-points that resulted in the greatest difference in Kaplan-Meier 5-Year EFS estimates between high, intermediate and low model score groups. These optimal cut-points were then carried over to the Discovery (Test) Cohort and AAML1031 Validation Cohort for validation. The cut-point to separate the high-risk patients was determined before the cut-point to separate the low risk patients.

To determine whether the predictor's prognostic ability was independent of established prognostic factors at diagnosis, multivariate Cox PH analysis was performed on model scores, risk group assignments, white blood cell (WBC) count status, HSCT status, and *FLT3*-ITD status.

Cell line

HEK-293 cells were maintained in Dulbecco's Modified Eagle Medium (DMEM; Life Technologies, Burlington ON) supplemented with 10% (v/v) fetal bovine serum (FBS; Life Technologies) in a 37°C incubator with a 5% humidified atmosphere.

Plasmid constructs and miRNA mimics

miRNA expression was increased using MIRIDIAN miRNA mimics (ThermoScientific, Waltham MA) directed against miR-106a-5p and negative control #2 (NC2; negative control against *C. elegans* cel-miR-239b). Mimics were resuspended in nuclease-free water at a stock concentration of 100 μ M. The genomic or mismatched sequences corresponding to the predicted binding sites to miR-106a-5p were synthesized (IDT Technologies; Coralville IA) and cloned into the XhoI/NotI restriction sites of the psiCHECK2 vector (Promega; Madison WI) directly downstream of the Renilla luciferase reporter gene and verified by DNA sequence analysis. The mismatched sequences are exactly complementary to the seven-nucleotide seed regions of the predicted miR-106a-5p binding site.

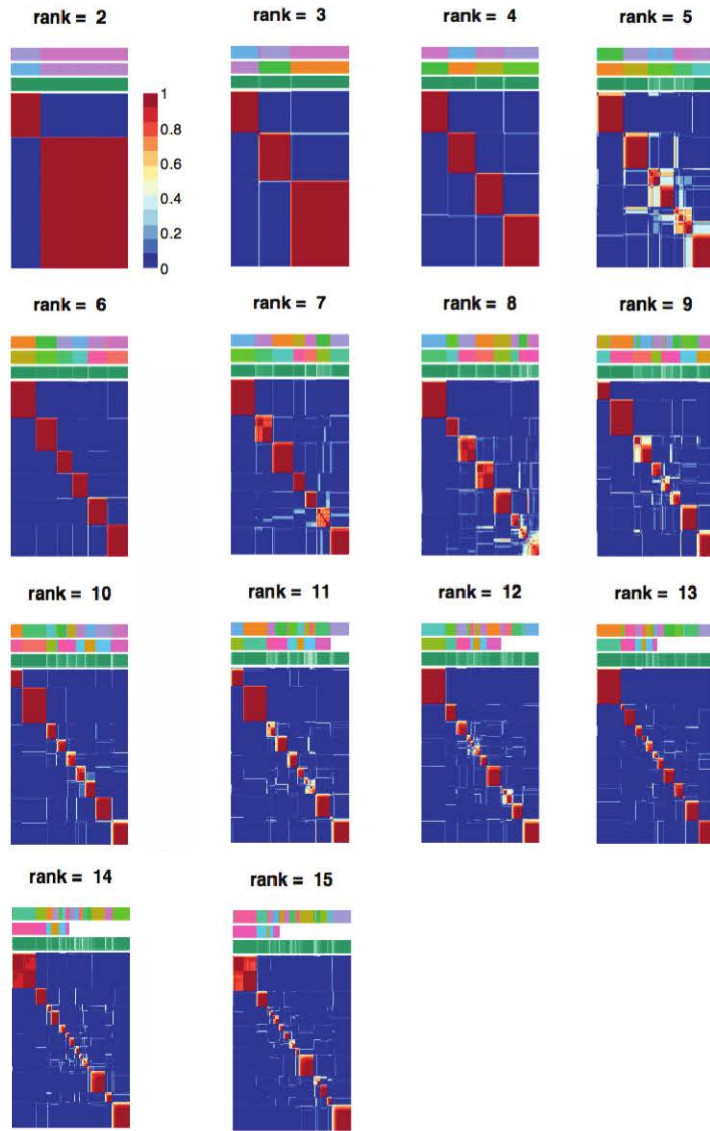
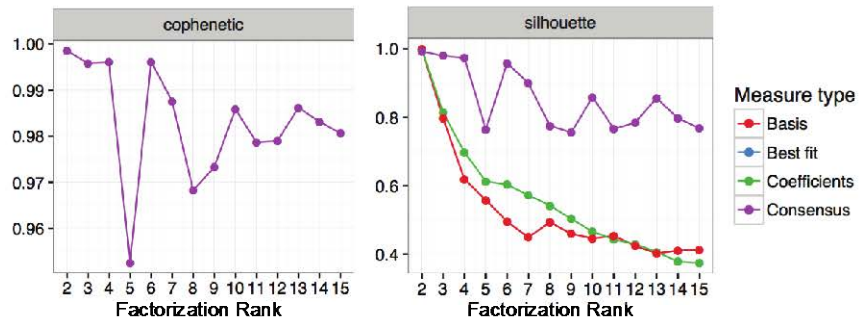
Dual-Luciferase reporter assays

Dual-Glo reporter assays were performed as previously described^{1, 5}. HEK-293 cells were seeded onto 24-well plates one day before transfection. Luciferase reporter constructs were co-transfected with miR-106a-5p or NC2 control mimics using TurboFect Transfection Reagent (ThermoScientific) in OPTI-MEM (Life Technologies) without FBS. Six hours following transfections, media were changed to DMEM supplemented with 10% FBS. 24h after transfections, cells were reseeded into 96-well plates. 48h after transfection, cells were lysed and luciferase activities were assayed using the Dual-Glo Luciferase Reporter Assay System (Promega). On the luciferase construct, Renilla luciferase was located downstream of the inserted miRNA binding site of interest and thus was used to monitor responses to miRNA over-expression, while the firefly luciferase was included on the plasmid as an intraplasmid transfection normalization reporter. As such, Renilla/Firefly luciferase ratios were calculated for each well to account for transfection efficiencies. These experiments were performed in triplicate and were shown as means \pm SEM. Statistical comparisons were performed using unpaired two-tailed t-tests with Bonferroni multiple-test correction, where significant differences were those with adjusted p-value < 0.05.

Supplementary Figures

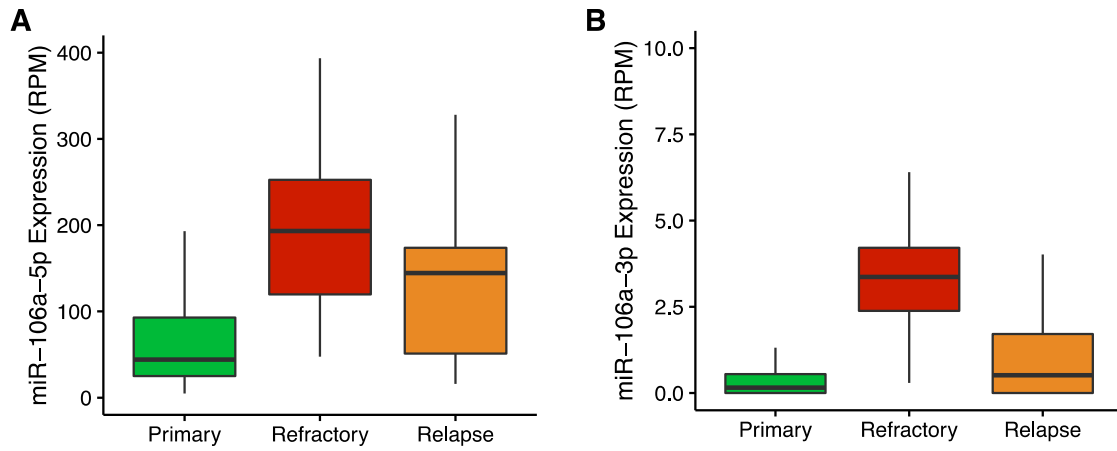
Supplementary Figure S1 – miRNA k2-15 NMF metrics.

A) Consensus maps of rank (k) 2-15 solutions of unsupervised clustering of miRNA expression profiles of 637 primary samples. Deep red blocks indicate samples that consistently cluster with one another. B) Cophenetic coefficients (that provide measurements of the stability of the clusters), and silhouette widths (that indicate the consistency of the membership of each sample in the assigned cluster) of k: 2-15 solutions. The k=4 solution was chosen as it had the second highest cophenetic coefficient, and we reasoned that studying 4 sub-groups (as opposed to 2 sub-groups) would uncover more insight into the heterogeneity of mRNA transcript expression in pediatric AML.

A**B**

Supplementary Figure S2 – miR-106a expression in the Discovery Cohort.

A) Boxplot depicting miR-106a-5p expression in primary, relapse and refractory samples. B) Boxplot depicting miR-106a-3p expression in primary, relapse and refractory samples.

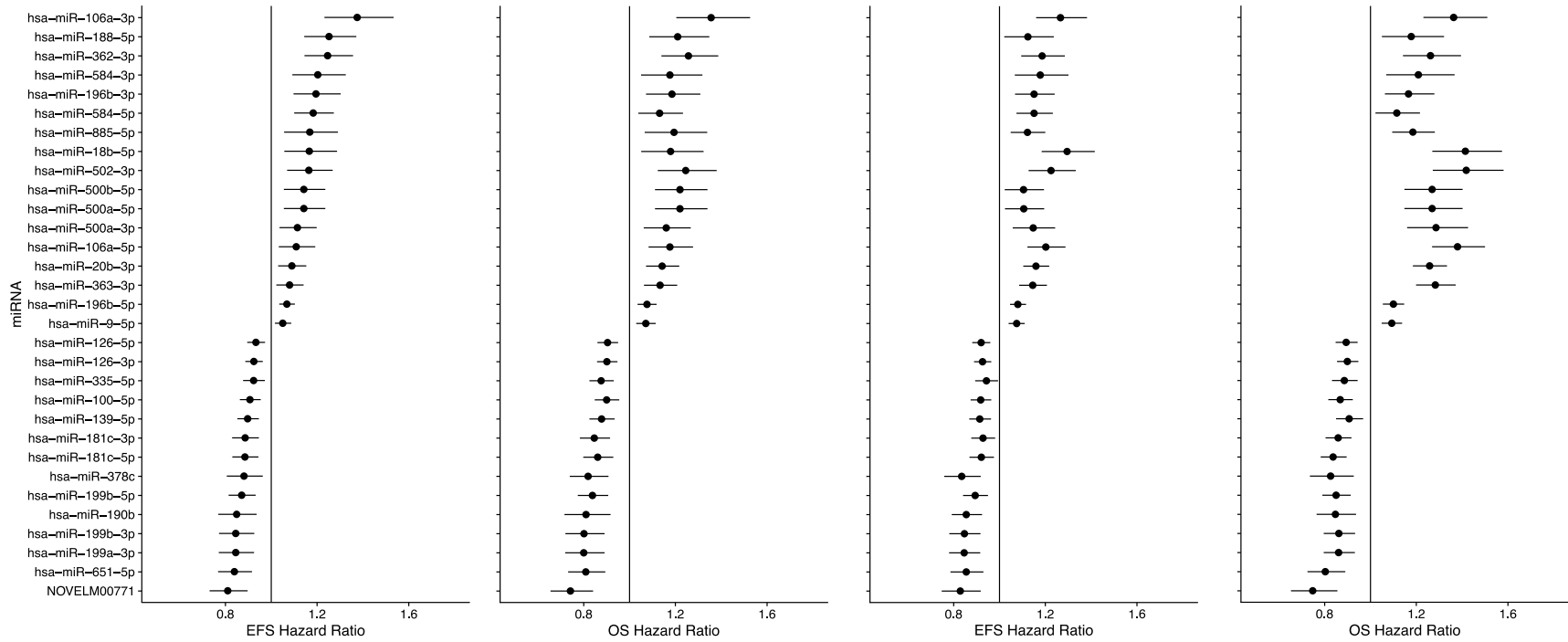


Supplementary Figure S3 – miRNA with linear associations with patient overall survival (OS) and event free survival (EFS) in both the Discovery Cohort and AAML1031 Validation Cohort

31 miRNAs had significant linear associations with overall survival (OS) and event free survival (EFS) in both the Discovery Cohort and AAML1031 Validation Cohort – 17 miRNAs were associated with superior outcomes and 14 other miRNAs were associated with inferior outcomes. Threshold for significance: Discovery Cohort – Univariate Cox PH q-value <0.05; AAML1031 Validation Cohort – Univariate Cox PH p-value <0.05. EFS and OS forest plots displaying Cox proportional hazard ratios and 95% confidence intervals of miRNAs that are significantly associated with survival in the Discovery Cohort (left) and AAML1031 Validation Cohort (right).

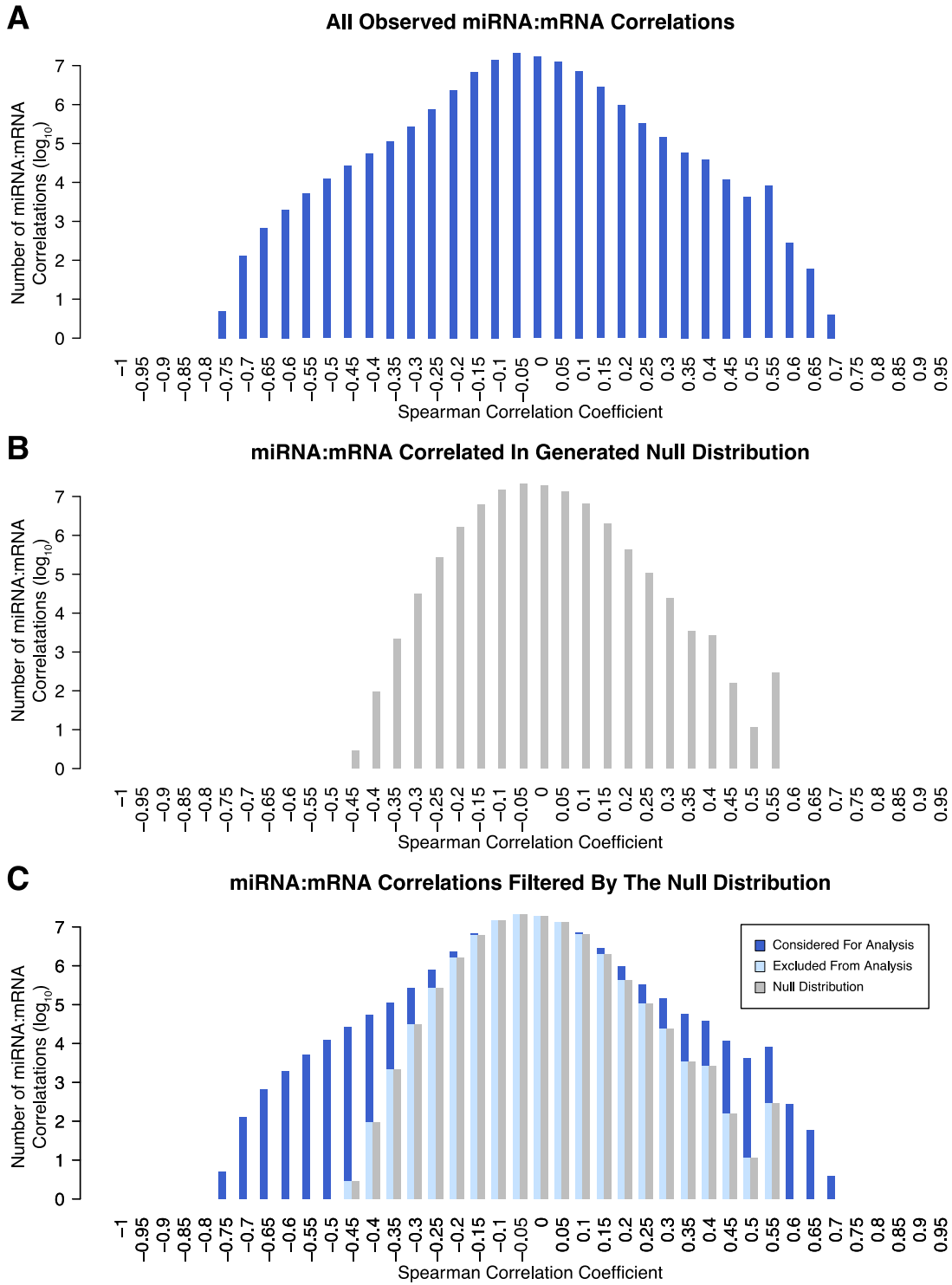
DISCOVERY COHORT (n=637)

AAML1031 VALIDATION COHORT (n=666)



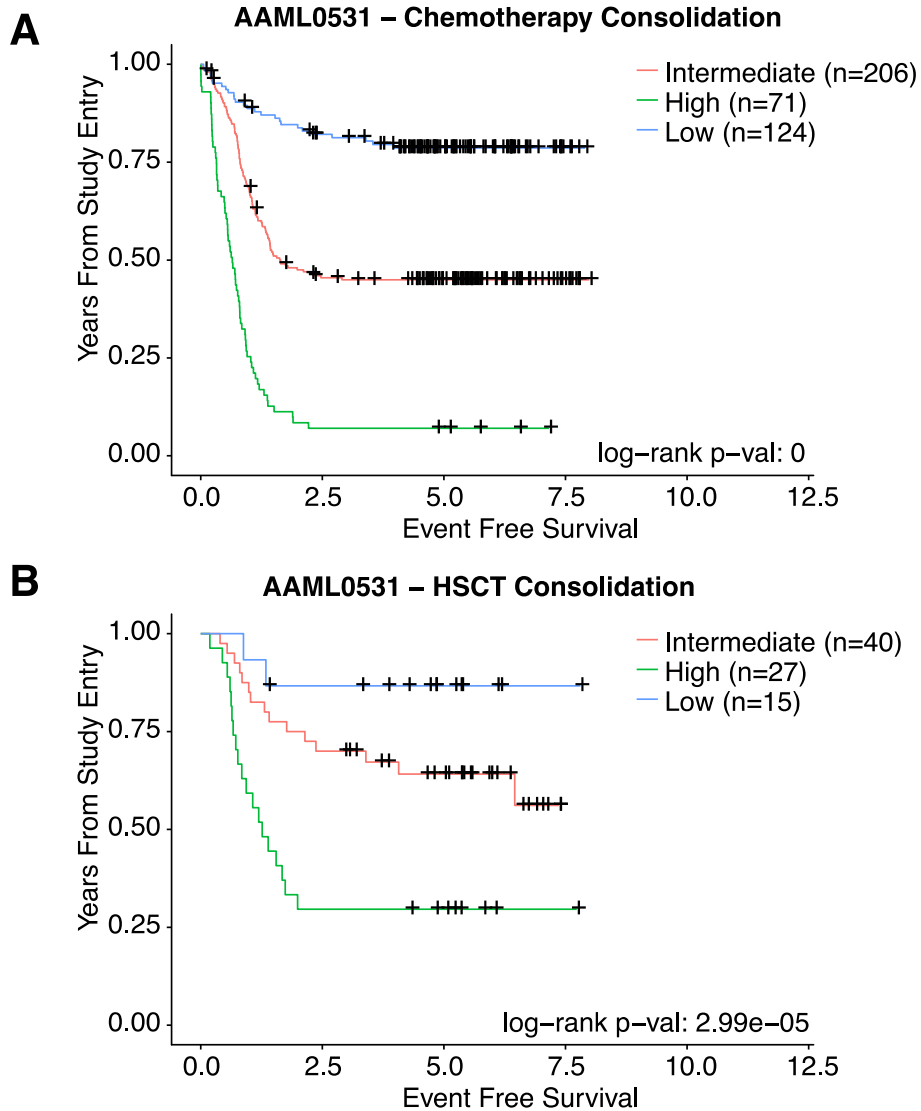
Supplementary Figure S4 – Identifying miRNA:mRNA expression correlations.

A) In order to identify miRNA:mRNA pairs with anti-correlated expression profiles, we performed Spearman correlation tests for each miRNA:mRNA pair. The resulting Spearman correlation coefficients are displayed in this histogram. B) In order to represent miRNA:mRNA correlations that are noise, we generated a null distribution consisting of Spearman correlation coefficients of scrambled data. The null distribution was derived by performing Spearman correlations 50 times, each time randomizing the miRNA-seq library IDs. The resulting Spearman correlation coefficients are displayed in this histogram. C) To account for correlations that might have been stochastic noise, the rho distribution was then divided in 40 bins and the counts for each bin compared with counts from the null distribution depicted in B. miRNA:mRNA pairs in each bin were sorted by adjusted p-value, and only those that ranked above the threshold set by counts from bins derived from null distribution were considered for further analysis. In this plot, the grey bars represent the null distribution, the dark blue bars represent miRNA:mRNA correlations that were considered for analysis, and light blue bars represent miRNA:mRNA correlations that were excluded for analysis because they were considered stochastic noise.



Supplementary Figure S5 – AAML0531 Patient EFS (Grouped By Consolidation Therapy)

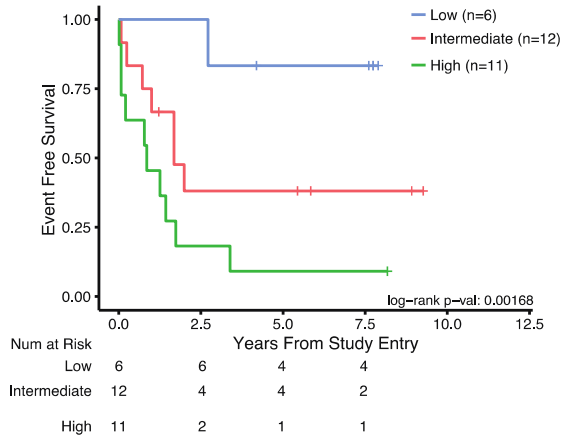
Kaplan Meier plots illustrating the utility of the miRNA-based EFS prognostic model on AAML0531 patients who received HSCT (A) and patients who did not (chemotherapy only) (B). Only patients for whom we had HSCT status data were considered.



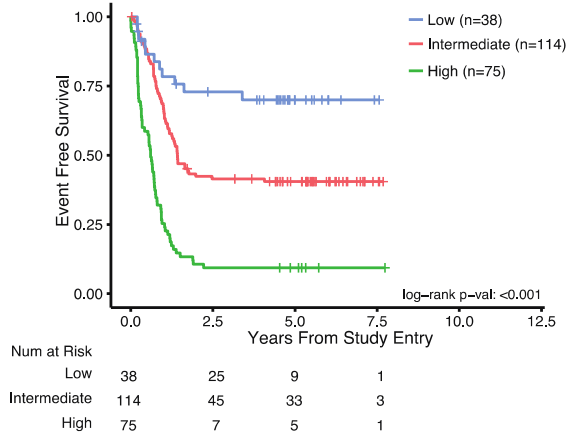
Supplementary Figure S6 – Cytogenetic/molecular Standard Risk cases are further classified by AMLmiR36

Kaplan-Meier plots displaying Standard Risk (by cytogenetic/molecular grouping) cases from each clinical trial (AAML03P1, AAML0531, AAML1031) stratified by AMLmiR36. The high AMLmiR36 group cases (represented by green lines) consistently have significantly inferior outcomes when compared with the intermediate AMLmiR36 group cases (represented by red lines).

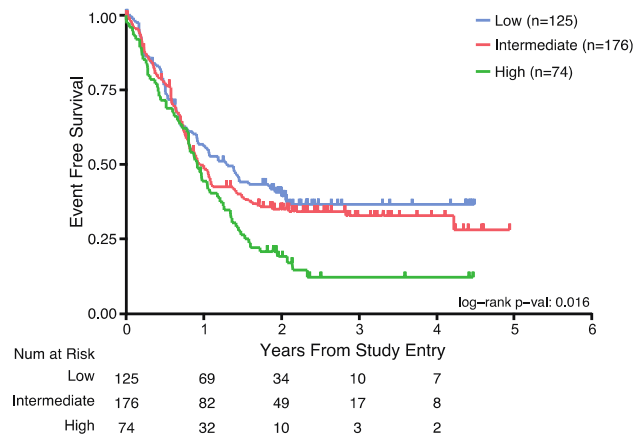
AAML03P1 – Standard Risk EFS



AAML0531 – Standard Risk EFS



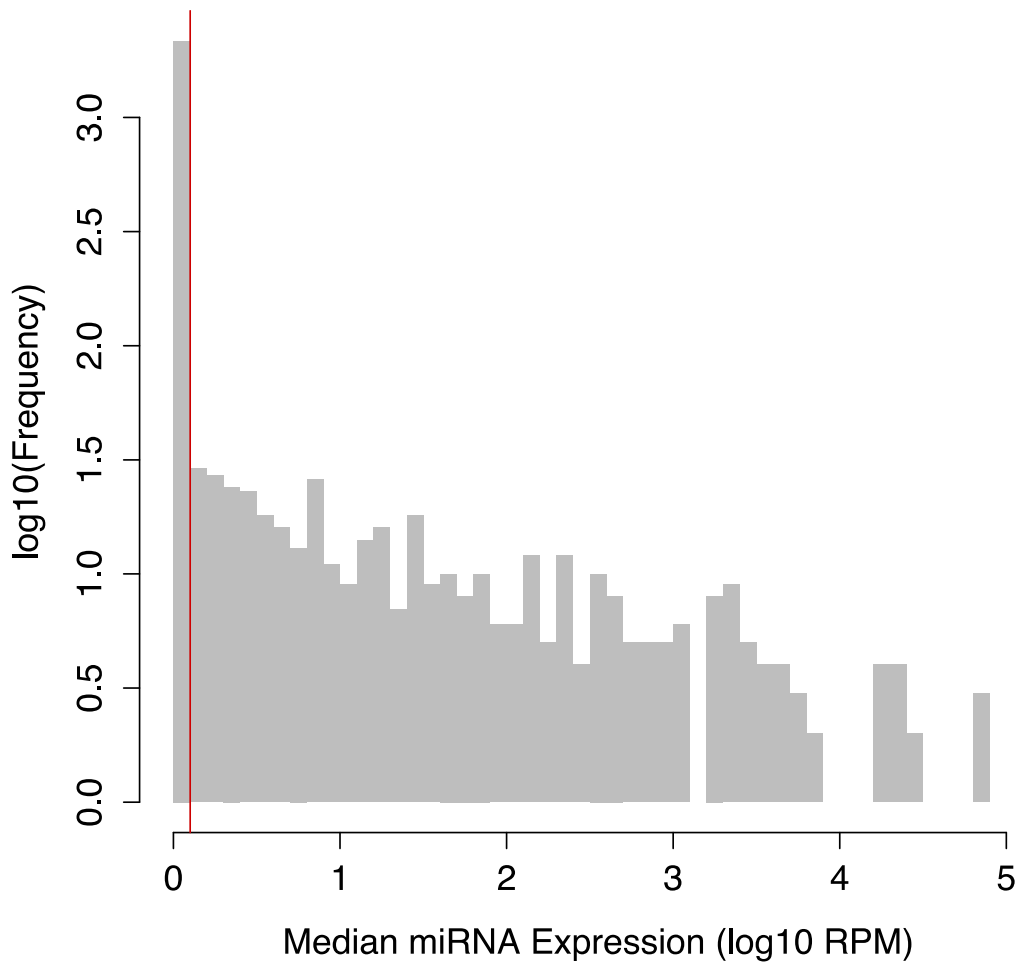
AAML1031 – Standard Risk EFS



Supplementary Figure S7 – Median miRNA Expression

Histogram of the median expression of each mirbase21 (n=2585) miRNA across 637 pediatric AML primary samples. Red line indicates 10RPM, the threshold for expressed miRNAs.

Histogram of Median miRNA Expression



References For Supplementary Information

1. Lim EL, Trinh DL, Scott DW, et al: Comprehensive miRNA sequence analysis reveals survival differences in diffuse large B-cell lymphoma patients. *Genome Biol* 16:18, 2015
2. Gams AS, Alonzo TA, Meshinchi S, et al: Gemtuzumab Ozogamicin in Children and Adolescents With De Novo Acute Myeloid Leukemia Improves Event-Free Survival by Reducing Relapse Risk: Results From the Randomized Phase III Children's Oncology Group Trial AAML0531. *J Clin Oncol*, 2014
3. Camp RL, Dolled-Filhart M, Rimm DL: X-tile: a new bio-informatics tool for biomarker assessment and outcome-based cut-point optimization. *Clin Cancer Res* 10:7252–7259, 2004
4. The Cancer Genome Atlas Research Network: Genomic and epigenomic landscapes of adult de novo acute myeloid leukemia. *N Engl J Med* 368:2059–2074, 2013
5. Trapnell C, Roberts A, Goff L, et al: Differential gene and transcript expression analysis of RNA-seq experiments with TopHat and Cufflinks. *Nat Protoc* 7:562–578, 2012